Journal of the European Ceramic Society xxx (xxxx) xxx–xxx

Contents lists available at ScienceDirect

Journal of the European Ceramic Society

journal homepage: www.elsevier.com/locate/jeurceramsoc

Original Article

Structure, microwave dielectric properties, and infrared reflectivity spectrum of olivine type Ca_2GeO_4 ceramic

Ying Tang[a,b], Minyu Xu[b], Lian Duan[b], Junqi Chen[b], Chunchun Li[c], Huaicheng Xiang[b], Liang Fang[b,*]

[a] Department of Physical Chemistry, University of Science and Technology Beijing, Beijing, 100083, China
[b] College of Materials Science and Engineering, Guilin University of Technology, Guilin, 541004, China
[c] College of Information Science and Engineering, Guilin University of Technology, Guilin, 541004, China

ARTICLE INFO

Keywords:
Olivine structure
Ca_2GeO_4 ceramic
Low-εr
High $Q\times f$
Infrared reflectivity spectrum

ABSTRACT

Ca_2GeO_4 dielectric ceramic was prepared using the conventional solid-state reaction method. Sintering behavior, crystal structure, microstructure, and microwave dielectric properties were analyzed by XRD, SEM, Raman, and Infrared reflectivity spectrum. Ca_2GeO_4 was found to crystallize in the olivine structure with a space group of *Pnma*. A dense and high-performance microwave dielectric property with permittivity ~ 6.76 ± 0.02, $Q\times f$ value ~ 82,400 ± 1800 GHz, and temperature coefficient ~ -67 ± 3.4 ppm/°C were obtained in the sample sintered at 1420 °C. Infrared spectral analysis supported that the dielectric contribution for Ca_2GeO_4 at microwave region is dominated by absorption of phonons and there is no contribution from dipolar or other polarization mechanisms. The large negative τ_f values could be compensated by forming composite ceramics with $CaTiO_3$. A low-ε_r of 9.02 ± 0.03, a high $Q\times f$ of 49,880 ± 1400 GHz, and a near-zero τ_f value of +4 ± 0.6 ppm/°C were obtained for $0.92Ca_2GeO_4$-$0.08CaTiO_3$ ceramic at 1420 °C for 4 h. This ceramic could be a good candidate for microwave substrate materials.

1. Introduction

Microwave dielectric ceramics as a kind of core materials for microwave devices (such as resonators, filters, substrates etc.) are widely used in intelligent transportation systems (ITS), radar, mobile phone and global positioning system (GPS) etc [1–3]. Commonly, the judgments of microwave properties have three prime requirements: the suitable dielectric constant ε_r, the high quality factor Q, and the stable temperature coefficient of resonant frequency (τ_f) [4,5]. The era of miniaturization, high frequency and integration of microwave dielectrics is coming. It means more powerful microwave substrates should be exploited, which could carry more components and exhibit better dielectric and thermal properties. Since the wavelength inside the devices is inversely proportional to the square root of its dielectric constant, the use of high ε_r materials can be beneficial to miniaturization, but high dielectric constant materials commonly increase the leakage current of integrated circuits, the capacitance effect between wires and the heating of integrated circuits. Nevertheless, the time of signal delay is proportional to the square root of dielectric constants, and the low-ε_r materials could enhance the transition speed, and decrease the heating and system loss during high working frequency transmission [6–10]. Thus, the low-ε_r, high-Q and thermal stability materials could be considered to be the most promising candidates for the next-generation substrates in high frequency electronic devices.

Up to now, the typical low-ε_r and high-Q microwave dielectric materials including Al-, Si-based materials, such as spinel structure MAl_2O_4 (M = Zn, Mg, Ni, Co) [11–13], olivine structure A_2SiO_4 (A = Ca, Mg) [14,15]. But, the sintering temperatures of Al-containing compounds are suitable to co-fired with the refractory metal electrode, such as W, Mo, which should be sintered with ceramics in the range of 1200–1600 °C with the reducing atmosphere, resulting in a more expensive cost and more difficult process. During these materials, some Si-containing olivine structure dielectric materials have attracted considerable attention, such as Mg_2SiO_4 (ε_r = 7.5, $Q\times f$ = 114,730 GHz, τ_f = −57 ppm/°C) [15]. As well-known, germanium and silicon are in the same group in the periodic table, and Ge atom has the same electrovalence and similar electronic shell structure to Si atom. Based on this, Chen et al. [16] first reported the Mg_2GeO_4 dielectric material with low-ε_r and high-Q. Furthermore, Eulenberger et al. reported the synthesis of olivine structure Ca_2GeO_4 in their optical studies and used it in laser material [17–19]. To date, the microwave dielectric properties of Ca_2GeO_4 have not been studied yet. Considering the excellent

* Corresponding author.
E-mail address: fanglianggl001@aliyun.com (L. Fang).

https://doi.org/10.1016/j.jeurceramsoc.2019.02.039
Received 19 December 2018; Received in revised form 16 February 2019; Accepted 19 February 2019

dielectric performances of Mg_2GeO_4, thus, it is reasonable to predict that Ca_2GeO_4 might possess promising microwave dielectric properties, and it is also worth to investigate the relationship between structure and microwave properties.

In this work, Ca_2GeO_4 ceramics were synthesized by the traditional solid-state reaction method. The relationships between sintering behavior, crystal structure, microstructure, and microwave dielectric properties were analysis by XRD, SEM, Raman, and infrared reflectivity spectrum in detail.

2. Experimental section

Ca_2GeO_4 ceramics were prepared by a conventional solid-state reaction method using high-purity powders of $CaCO_3$ (99.99%, Guo-Yao Co. Ltd., China) and GeO_2 (99.99%, Guo-Yao Co. Ltd., China) as the raw materials. The weighted powers were ball-milled for 4 h, dried, and calcined at 1250 °C for 4 h. The calcined powders were re-milled for 4 h with PVA as binders. The granulated powders were then pressed into cylinders (10 mm in diameter and 6 mm in thickness) in a steel die under uniaxial pressure of 200 MPa. The samples were heated at 550 °C for 4 h to remove the organic binders and sintered at 1350–1440 °C for 4 h at a rate of 5 °C/min and naturally cooled to the room temperature. The thin pellet was prepared for room temperature infrared reflectivity spectra measurement.

The relative densities of the sintered samples were measured with the Archimede's method. The phase purity of the fired ceramics was investigated using an X-ray diffractometer (XRD; Model X'Pert PRO, PANalytical, Almelo, the Netherlands). The microstructures of the samples were examined by field-emission scanning electron microscopy (FESEM; S4800, Hitachi, Tokyo, Japan). The Raman spectra at room temperature were obtained with a Raman spectrometer (DXR; Thermo Fisher Scientific, American). Microwave dielectric properties of the sintered ceramics were measured using a network analyzer (N5230 A, Agilent Co., Palo Alto, California) and a temperature chamber (Delta 9039, Delta Design, San Diego, California). The τ_f values were obtained in the temperature range of 25 °C–85 °C:

$$\tau_f = \frac{f2 - f1}{f1(T2 - T1)} \quad (1)$$

where, f_1 and f_2 represent resonant frequencies at temperatures T_1 and T_2, respectively.

The room-temperature infrared reflectivity spectra of the pellet with the surface carefully polished were measured using a Bruker IFS 66v FTIR spectrometer on Infrared beamline station at National Synchrotron Radiation Lab. (NSRL), China. The resolution of the spectrum was selected as 2 cm^{-1} and the incident angle of radiation was fixed at 12°. The spectrum in the frequency range of 50–4000 cm^{-1} was obtained by the combination of the two spectra in the frequency ranges of 50–600 and 400–4000 cm^{-1}. In the former range, an FIR-DTGS far-infrared-deuterated triglycine sulfate detector and Mylar multilayer film beam splitter (total thickness of 6 μm) were employed, while in the latter range, the FIR-DTGS detector and Ge/KBr beam splitter were employed. The far-infrared reflection spectra of Ca_2GeO_4 ceramics were collected in the wavenumber range from 50 cm^{-1} to 1000 cm^{-1}, and were analyzed using a classical harmonic oscillator model (the Lorentz three parameter classical model) [20]:

$$\varepsilon^*(\omega) = \varepsilon_\infty + \sum_{j=1}^{n} \left(\frac{\omega_{pj}^2}{\omega_{oj}^2 - \omega^2 - j\gamma_j\omega} \right) \quad (2)$$

where ε_∞ is the dielectric constant caused by the electronic displacive polarization at optical frequencies; γ_j, ω_{oj}, and ω_{pj} are the damping factor, the transverse frequency, and plasma frequency of the jth Lorentz oscillator, respectively, and n is the number of transverse phonon modes. The contribution to dielectric permittivity of each oscillator $\Delta\varepsilon_j$ i.e. strength is calculated as the ratio of $(\omega_{pj})^2$ to $(\omega_{oj})^2$. The reflectivity

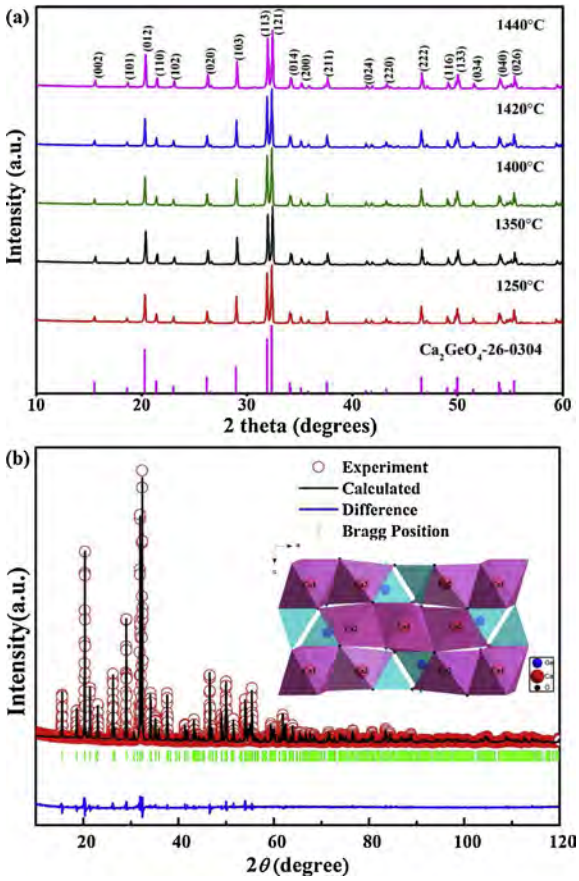

Fig. 1. (a) The XRD patterns of Ca_2GeO_4 powder prepared at 1250 °C and sintered at 1350–1440 °C; (b) the refinement of the Ca_2GeO_4 ceramics sintering at 1420 °C. The inset is the crystal structure of Ca_2GeO_4.

R(ω) can be calculated from the complex dielectric function as according to [21]:

$$R(\omega) = \left| \frac{1 - \sqrt{\varepsilon^*(\omega)}}{1 + \sqrt{\varepsilon^*(\omega)}} \right|^2 \quad (3)$$

3. Results and discussion

Fig. 1 shows the XRD patterns of Ca_2GeO_4 prepared and sintered at different sintering temperatures (1250–1440 °C). By indexing with the standard PDF card (#26-0304), no additional peaks were detected at 1250 °C. All existing peaks in samples sintered at 1350, 1400, 1420 and 1440 °C are related to Ca_2GeO_4 (PDF card #26-0304) without any additional phases. Based on the results of phase analysis, Rietveld refinement was performed on the sintered sample at 1420 °C using the Fullprof software with olivine-type Ca_2GeO_4 as the structural model. And Ca_2GeO_4 (ICSD #26-0304) as a starting model for the Rietveld refinement, the symbols represent the experimental data and the solid line could be satisfactorily fitting to the diffraction data which suggested the Ca_2GeO_4 powders (sintering at 1420 °C) crystallized in an orthorhombic olivine structure with a space group of *Pnma*, a = 11.3997 Å, b = 6.7919 Å, c = 5.2400 Å, $\alpha = \beta = \gamma = 90°$, and acceptable R_p = 4.11%, R_{wp} = 5.82%, and R_{exp} = 3.16%, χ^2 = 3.39. The inset of Fig. 1(b) was the olivine crystal structure for Ca_2GeO_4 ceramic. All the ions adopt the olivine structure and the unit cell of Ca_2GeO_4 consists of nine CaO_6 octahedral and six GeO_4 tetrahedral [22].

Fig. 2 shows the SEM images of the Ca_2GeO_4 ceramics sintered at various temperatures. At low sintering temperature (1350 °C) the

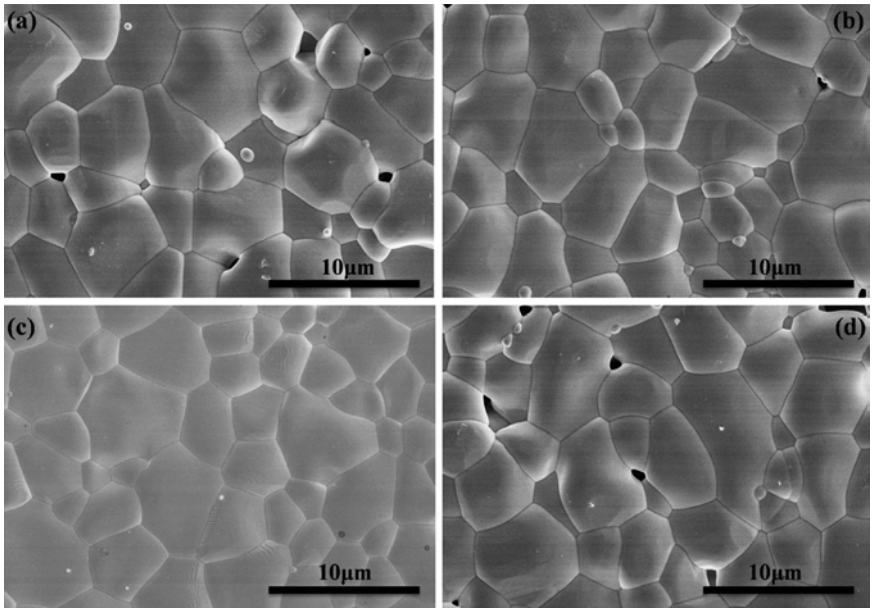

Fig. 2. The SEM images of the Ca_2GeO_4 ceramics sintered at different temperatures: (a) 1350 °C; (b) 1400 °C; (c) 1420 °C; (d) 1440 °C.

Table 1
The microwave dielectric properties (ε_r, $Q \times f$, and τ_f), bulk density and FWHW of the Ca_2GeO_4 ceramics sintered at 1350–1440 °C.

S.T. (°C)	ε_r	$Q \times f$ (GHz)	τ_f (ppm/°C)	Density (g/cm^3)	Relative density (%)	FWHM
1350	6.60 ± 0.05	58,100 ± 2,900	−66 ± 2.7	3.15 ± 0.03	89.2	6.03
1400	6.67 ± 0.02	74,630 ± 2,700	−65 ± 3.2	3.30 ± 0.02	93.4	5.99
1420	6.76 ± 0.02	82,400 ± 1800	−67 ± 3.4	3.35 ± 0.02	94.9	5.68
1440	6.59 ± 0.03	67,900 ± 2,000	−66 ± 2.5	3.28 ± 0.02	92.9	6.19

Ca_2GeO_4 ceramic exhibited a small amount of pores. However, when the sintering temperature increased to 1420 °C, the Ca_2GeO_4 ceramic exhibited a relatively dense microstructure and few visible pores (Fig. 2(c)). As the sintering temperature increased to 1440 °C, abnormal large grains (~11 μm) grains were overgrown and some pores re-occurred, which due to the excessive sintering temperature. The bulk densities of the sintered samples are listed in Table 1. As the sintering temperature increased, the bulk density just slightly increased from 3.15 g/cm^3 at 1350 °C, to a maximum value of 3.35 g/cm^3 at 1420 °C (~94.9% of the theoretical density), and then decreased to 3.28 g/cm^3 at 1440 °C. This decline in density might be ascribed to the formation of pores associated with several abnormal grain growths and a small amount of porosity at 1440 °C. Table 1 also lists the microwave dielectric properties (ε_r, $Q \times f$, and τ_f) of the Ca_2GeO_4 ceramics sintered at 1350–1440 °C. The optimum microwave dielectric properties with $\varepsilon_r = 6.76 \pm 0.02$, $Q \times f = 82{,}400 \pm 1800$, and $\tau_f = -67 \pm 3.4$ ppm/°C were obtained when sintered at 1420 °C. With the variation of sintering temperatures, microwave dielectric properties and densities have a similar trend, where the maximum values were obtained correspondingly with the maximal densities. It is well known that the ε_r was depended on density, icon polarizability, and secondary phase. Considering the effect of density, the porosity-corrected permittivity ($\varepsilon_{corrected}$) was calculated by the Bosman-Having's equation [23].

$$\varepsilon_{corrected} = \varepsilon_r (1 + 1.5p) \quad (4)$$

where, p is the fractional porosity. The $\varepsilon_{corrected}$ value for Ca_2GeO_4 ceramics sintered at 1420 °C is 7.34, which is slightly higher than the calculated theoretical permittivity ε_{theo} (~6.83) of Ca_2GeO_4 calculated by the Clausius-Mosotti equation [24].

Usually, $Q \times f$ values would be influenced by the extrinsic and intrinsic factors in microwave frequency range. The extrinsic losses are mainly attributed to the lattice defects, including second phases, oxygen vacancies, grain boundaries, and densification or porosities, which could be effectively reduced by optimizing the preparation parameters. According to the XRD results, the effects of the secondary phase could be neglected due to the absence of detection of secondary phases, and the variation of densification of Ca_2GeO_4 with sintering temperature has the similar change tendency as $Q \times f$ values, thus, sintering temperature and densification might be the main extrinsic reason for the change of $Q \times f$ value in Ca_2GeO_4 ceramics.

Some A_2BO_4-type olivine ceramics and their microwave dielectric properties are given in Table 2. As can be seen, these A_2BO_4-type dielectric ceramics have some similar characteristics, such as high sintering temperature, high $Q \times f$, low ε_r, and negative τ_f. Comparing to other olivine structure materials, Ca_2GeO_4 has a much higher $Q \times f$ value than that of $Li_2A'BO_4$ (A' = Zn, Mg; B = Ge, Si), but slightly lower than Mg_2SiO_4 and Mg_2GeO_4 [10,14–16,25–27]. The property difference might be due to the local structure variance induced by different atomic

Table 2
Microwave dielectric properties of some A_2BO_4-type ceramics with olivine structure.

Ceramics	S.T. (°C)	ε_r	$Q \times f$ (GHz)	τ_f (ppm/°C)	Reference
Li_2MgSiO_4	1250	5.1	15,380	/[a]	[25]
Li_2MgGeO_4	1220	6.1	28,500	−74.7	[10]
Ca_2GeO_4	1420	6.76	82,400	−67	This work
Li_2ZnGeO_4	1200	6.5	35,400	−60.6	[10]
$(Zn_{0.95}Co_{0.05})_2SiO_4$	1200	6.5	57,000	−55.0	[26]
Mg_2GeO_4	1250	6.76	95,000	−28.7	[16]
Mg_2SiO_4	1550	7.5	114,730	−59	[15]
Mg_2SnO_4	1600	8.41	55,100	−62	[27]
Ca_2SiO_4	1450	10.1	26,000	−89	[14]

[a] Not studied.

occupation [28,29]. Redhammer et al. [22]. have reported that the different size of the M1 cation (this position is equal to Ca1 in Ca_2GeO_4) might change the polyhedral distortion, expressed by the parameters bond-length distortion, octahedral angle variance, and octahedral quadratic elongation, and the Ca germanate olivine compounds generally have more regular octahedra than the analogous silicates. Moreover, the intrinsic loss is sensitive to crystal structure, which is affected by the vibration mode of the lattice, packing fraction, magnetic loss, and structure tilting [30,31]. Therefore, the intrinsic dielectric loss of Ca_2GeO_4 would be explored by the Raman spectrum and infrared reflectivity spectrum in the following part.

In general, the longer dimensional range associated with diffraction phenomena restricts the prediction of the variation in the local bonding characteristics through powder X-ray diffraction measurements. The Raman spectrum is very sensitive to the nature of bonding, and it is helpful to identify the characterizing of the local structure. According to the group theoretical method [32], there are 36 Raman active optical phonon modes, but the Ca_2GeO_4 ceramics observed in the Raman spectra are only 16–22 peaks, which is less than the theoretically expected Raman active modes. This phenomenon might be arising from the mutual influence of the mixed or overlapped Raman active vibration modes and resolution of the measuring instrument as well as the partial symmetry of the sample being destroyed, and many modes cannot be separated from one another at the spectral resolution employed.

The room-temperature Raman spectra of Ca_2GeO_4 ceramics sintered at different temperatures (1350, 1400, 1420, and 1440 °C) are presented in Fig. 3. The Raman in the range of 600–1000 cm^{-1} are assigned to stretching modes of the GeO_4 tetrahedra in the structure, and the strongest peak was assigned to the stretching vibration of GeO_4 tetrahedron [33], which was actually the symmetric Ge-O stretching mode (A_g symmetry) in GeO_4 tetrahedron; the bands observed in the range of medium range were associated with antisymmetric bending vibrations of GeO_4 tetrahedra. And the mode below 200 cm^{-1} is associated with the translational lattice motions of the Ca^{2+} cations [34]. Bending vibrations would be expected at lower frequency, but separating these from vibrations involving cations or lattice modes is difficult because of the occurrence of modes coupling and modes.

For a Raman mode, the FWHM is inversely correlated to the lifetime of the phonon, and usually, the narrower peak corresponds to the longer lifetime of phonon and less interaction with phonons [35]. These interactions would consume more energy, thereby decreasing the intrinsic dielectric loss and leading the microwave ceramic shows a low dielectric loss. The FWHM of Ca_2GeO_4 ceramic at the strongest Raman mode are listed in Table 1, the relative lower FWHM of Ge-O stretching mode with have a relative dielectric loss, which has a similar rule as the $Q \times f$ value.

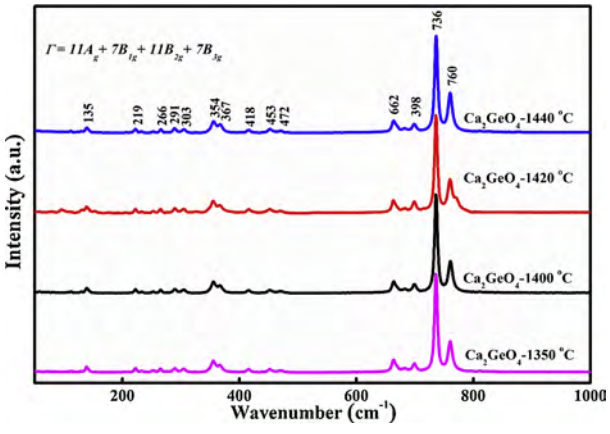

Fig. 3. The room-temperature Raman spectra of Ca_2GeO_4 ceramics sintered at different temperatures (1350–1440 °C).

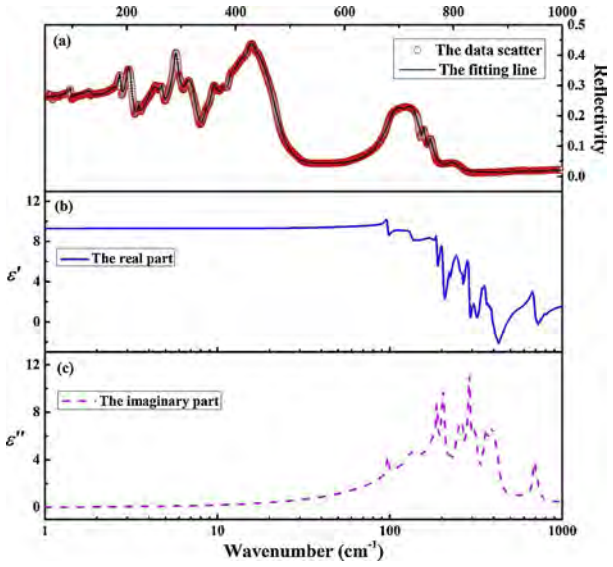

Fig. 4. The measured and calculated infrared reflectivity spectra of the Ca_2GeO_4 ceramics, (a) black solid lines is fitting values and red circles for measured values; (b)the blue solid is the real part; the pink line is the imaginary part. (For interpretation of the references to colour in this figure legend, the reader is referred to the web version of this article).

To further study the intrinsic microwave dielectric properties, the analysis based on infrared reflectivity spectra of the Ca_2GeO_4 were necessary as the infrared reflection spectra are mainly caused by the absorption of the polar lattice vibration. All calculated IR reflectivity spectrum of Ca_2GeO_4 was fitted well by 24 resonant modes though Eqs. (2)–(3), it is difficult to obtain all the independent peaks due to the instrumental resolution and interactions among these modes. The fitted spectra are in good agreement with the experimental ones, all of these data could be observed in Fig. 4 and Table 3. The spectrum data in the ranges of 0–50 cm^{-1} and 1000–5000 cm^{-1} without IR peaks were not considered to avoid instability, which may be caused by multiple reflections inside the grains and other unexpected effects. In order to represent more details, only the region with the frequency below

Table 3
The fitting parameters of vibration modes of $Ca_2Ge_2O_4$.

ω_{oj}(cm^{-1})	ω_{pj}(cm^{-1})	γ_j	$\Delta\varepsilon_j$
97.089	21.907	3.2004	0.0509
160.81	290.73	152.47	3.27
181.04	110.67	30.992	0.374
187.38	49.857	4.1671	0.0708
203.43	114.07	10.473	0.314
222.34	28.875	3.6472	0.0169
253.25	197.95	33.58	0.611
264.17	42.804	4.9092	0.0263
286.87	168.91	20.791	0.347
288.78	78.698	6.3809	0.0743
312.05	188.1	29.338	0.363
345.86	65.116	11.133	0.0354
358.95	149.91	17.354	0.174
375.12	132.37	20.982	0.125
389.84	81.91	11.664	0.0441
403.31	288.97	46.059	0.513
422.51	66.272	15.001	0.0246
442.82	71.177	38.665	0.0258
576.57	254.13	213.82	0.194
688.59	293.5	40.664	0.182
715.29	140.52	33.251	0.0386
743.39	32.836	4.9484	0.00195
755.47	36.027	6.225	0.00227
796.17	73.868	24.626	0.00861
ε_∞ = 1.88			

Table 4
Microwave dielectric properties of $(1-x)Ca_2GeO_4$-$xCaTiO_3$ composites sintered at different temperatures.

x values	S.T.(°C)	ε_r	$Q \times f$ (GHz)	τ_f (ppm/°C)
0	1420	6.76 ± 0.02	82,400 ± 1800	−67 ± 3.4
0.02	1390	7.25 ± 0.03	53,580 ± 2,500	−45 ± 2.5
0.04	1400	7.72 ± 0.03	51,300 ± 1,900	−23 ± 1.5
0.06	1410	8.26 ± 0.04	50,460 ± 1,600	−10 ± 1.3
0.08	1420	9.02 ± 0.03	49,880 ± 1400	+4 ± 0.6
0.10	1430	9.43 ± 0.05	48,040 ± 1300	+25 ± 1.5

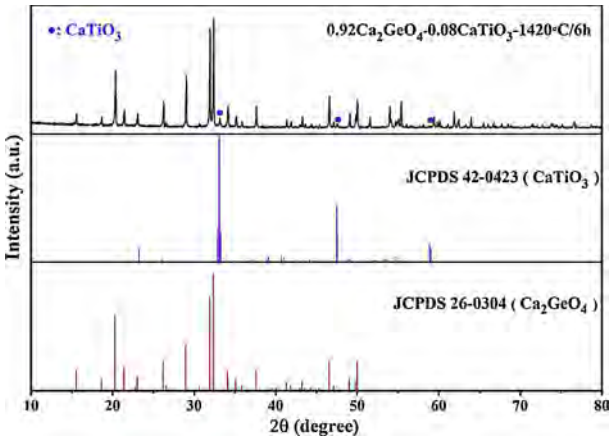

Fig. 5. The XRD patterns of $0.92Ca_2GeO_4$-$0.08CaTiO_3$ ceramics.

1000 cm^{-1} is displayed. The fitted parameters are listed in Table 3. The phonon parameters illustrate that the dielectric constant can reach 6.89 and contribute mainly (above 78.56%) to the dielectric polarization at microwave frequencies, which are below 800 cm^{-1}, and the calculated $Q \times f$ value was 134,198 GHz using Eq. (4). But it is difficult to calculate every contribution to the polarization from each vibrational mode at microwave frequencies. It is seen that the calculated permittivity (ε_r = 8.768) are slightly larger than the experimental one (ε_r = 6.76) in the microwave region, it could be concluded that the polarization is dominated by absorption of phonons at the far infrared region and that there is no contribution from dipolar or other polarization mechanisms [36]. But the calculated $Q \times f$ values is higher than the measured values, which means extrinsic loss and intrinsic loss might be influenced on $Q \times f$ values in the microwave range, thus, it is possible to enhance the $Q \times f$ values by optimizing the preparation processes.

In order to satisfy the requirements of electronic devices, microwave dielectric materials should have a near-zero τ_f value. In general, two main methods are proposed to improve the τ_f value. The first method is the formation of a composite between two compounds with opposite signs of τ_f value, for example, the addition of TiO_2 with τ_f = +450 ppm/°C can adjust the negative τ_f, such as in $(1-x)ZnZrNb_2O_8$-$xTiO_2$, $(1-x)ZnMoO_4$-$xTiO_2$ [37,38]. The second accepted method to obtain a near-zero τ_f value is forming solid solution phases. This method is desirable owing to its ability to maintain the high $Q \times f$ while successfully tuning the τ_f value. More recently, the $CaTiO_3$ ceramic with a large positive τ_f ~ +800 ppm/°C was prepared and characterized [39]. Therefore, $CaTiO_3$ was used to improve the τ_f values of Ca_2GeO_4 ceramics. Table 4 shows the microwave dielectric properties of $(1-x)Ca_2GeO_4$-$xCaTiO_3$ ceramics sintered at different temperatures (1390–1430 °C). Temperature stable ceramics with a near-zero τ_f value (+4 ± 0.6 ppm/°C) for $0.92Ca_2GeO_4$-$0.08CaTiO_3$ were obtained.

XRD pattern of $0.92Ca_2GeO_4$-$0.08CaTiO_3$ ceramic is shown in Fig. 5. From the XRD patterns, only the peaks of Ca_2GeO_4 and $CaTiO_3$ (JCPDS No. 042-0423) could be detected without any other secondary phase, indicating that Ca_2GeO_4 and $CaTiO_3$ ceramics did not react at 1420 °C.

4. Conclusion

In this work, Ca_2GeO_4 ceramics with orthorhombic olivine structure were synthesized by the conventional solid-state reaction route. The optimum microwave dielectric properties of Ca_2GeO_4 ceramics with ε_r = 6.76 ± 0.02, $Q \times f$ = 82,400 ± 1800 GHz, and τ_f = -67 ± 3.4 ppm/°C were obtained when sintered at 1420 °C. According to the result of infrared reflectivity, the polarization is dominated by absorption of phonons at the far infrared region, which is not affected by dipolar or other polarization mechanisms. The large negative τ_f values could be compensated by forming composite ceramics, a near zero τ_f values of +4 ± 0.6 ppm/°C were obtained for $0.92Ca_2GeO_4$-$0.08CaTiO_3$ ceramic sintered at 1420 °C for 4 h. The olivine structure Ca_2GeO_4 could be a promising candidate for microwave substrate materials.

Acknowledgments

This work was supported by Natural Science Foundation of China (Nos. 21761008 and 21561008), the Natural Science Foundation of Guangxi Zhuang Autonomous Region (Nos. 2016GXNSFBA380134, and 2015GXNSFFA139003, 2018GXNSFAA138175, 2018GXNSFAA281093), and Projects of Education Department of Guangxi Zhuang Autonomous Region (No. 2018KY0255). The authors would also like to thank the administrators in the IR beamline workstation of National Synchrotron Radiation Laboratory (NSRL) for their help in the IR measurements.

References

[1] M.T. Sebastian, R. Ubic, H. Jantunen, Low-loss dielectric ceramic materials and their properties, Int. Mater. Rev. 60 (2015) 392–412.
[2] K. Du, X.Q. Song, J. Li, J.M. Wu, W.Z. Lu, X.C. Wang, W. Lei, Optimised phase compositions and improved microwave dielectric properties based on calcium tin silicates, J. Eur. Ceram. Soc. 39 (2019) 340–345.
[3] Y. Tang, X. Jiang, H. Xiang, C. Li, L. Fang, X. Xing, Two novel low-firing $Na_2AMg_2V_3O_{12}$ (A = Nd, Sm) ceramics and their chemical compatibility with silver, Ceram. Int. 43 (2017) 2892–2898.
[4] D. Zhou, L.X. Pang, D.W. Wang, C. Li, B.B. Jin, I.M. Reaney, High permittivity and low loss microwave dielectrics suitable for 5G resonators and low temperature co-fired ceramic architecture, J. Mater. Chem. C 5 (2017) 10094–10098.
[5] H. Xiang, C. Li, H. Jantunen, L. Fang, A.E. Hill, Ultralow loss $CaMgGeO_4$ microwave dielectric ceramic and its chemical compatibility with silver electrodes for low-temperature cofired ceramic applications, ACS Sustain. Chem. Eng. 6 (2018) 6458–6466.
[6] Y. Tang, W. Fang, L. Fang, C. Li, Phase transformation and microwave dielectric properties of $Ba_4LiTa_{3-x}Sb_xO_{12}$, Ceram. Int. 41 (2015) 6653–6656.
[7] D. Zhou, C.A. Randall, L.X. Pang, H. Wang, J. Guo, G.Q. Zhang, Y. Wu, K.T. Guo, L. Shui, X. Yao, Microwave dielectric properties of $(ABi)_{1/2}MoO_4$ (A = Li, Na, K, Rb, Ag) type ceramics with ultra-low firing temperatures, Mater. Chem. Phys. 129 (2011) 688–692.
[8] M. Rakhi, G. Subodh, Crystal structure and microwave dielectric properties of $NaPb_2B_2V_3O_{12}$ (B = Mg, Zn) ceramics, J. Eur. Ceram. Soc. 38 (2018) 4962–4966.
[9] C. Yin, H. Xiang, C. Li, H. Porwal, L. Fang, Low-temperature sintering and thermal stability of Li_2GeO_3-based microwave dielectric ceramics with low permittivity, J. Am. Ceram. Soc. 101 (2018) 4608–4614.
[10] C. Li, H. Xiang, M. Xu, Y. Tang, L. Fang, Li_2AGeO_4 (A = Zn, Mg): two novel low-permittivity microwave dielectric ceramics with olivine structure, J. Eur. Ceram. Soc. 38 (2018) 1524–1528.
[11] C.W. Zheng, S.Y. Wu, X.M. Chen, K.X. Song, Modification of $MgAl_2O_4$ microwave dielectric ceramics by Zn substitution, J. Am. Ceram. Soc. 90 (2007) 1483–1486.
[12] C.L. Huang, C.Y. Tai, C.Y. Huang, Y.H. Chien, Low-loss microwave dielectrics in the spinel-structured $(Mg_{1-x}Ni_x)Al_2O_4$ solid solutions, J. Am. Ceram. Soc. 93 (2010) 1999–2003.
[13] W.C. Tsai, Y.H. Liou, Y.C. Liou, Microwave dielectric properties of $MgAl_2O_4$-$CoAl_2O_4$ spinel compounds prepared by reaction-sintering process, Mater. Sci. Eng. B 177 (2012) 1133–1137.
[14] T. Joseph, M.T. Sebastian, Microwave dielectric properties of alkaline earth orthosilicates M_2SiO_4 (M = Ba, Sr, Ca), Mater. Lett. 65 (2011) 891–893.
[15] K.X. Song, X.M. Chen, X.C. Fan, Effect of Mg/Si ratio on microwave dielectric characteristics of forsterite ceramics, J. Am. Ceram. Soc. 90 (2007) 1808–1811.
[16] C.X. Chen, S.P. Wu, Y.X. Fan, Synthesis and microwave dielectric properties of B_2O_3-doped Mg_2GeO_4 ceramics, J. Alloys. Compd. 578 (2013) 153–156.
[17] G. Eulenberger, A. Wittmann, H. Nowotny, Germanate mit zweiwertigen Metallionen, Monatshefte für Chemie und verwandte Teile anderer Wissenschaften 93 (1962) 1046–1054.
[18] C. Li, J. Xu, W. Liu, D. Zheng, S. Zhang, Y. Zhang, H. Lin, J. Liu, F. Zeng, Synthesis and characterization of Cr^{4+}-doped Ca_2GeO_4 tunable crystal, J. Alloys. Compd. 636

(2015) 211–215.
[19] Z. Jiang, Y. Wang, Z. Ci, H. Jiao, Electronic structure and luminescence properties of yellow-emitting Ca_2GeO_4: Ce^{3+}, Li^+ phosphor for white light-emitting diodes, J. Electrochem. Soc. 156 (2009) J317–J320.
[20] J. Chen, Y. Tang, H. Xiang, L. Fang, H. Porwal, C. Li, Microwave dielectric properties and infrared reflectivity spectra analysis of two novel low-firing $AgCa_2B_2V_3O_{12}$ (B = Mg, Zn) ceramics with garnet structure, J. Eur. Ceram. Soc. 38 (2018) 4670–4676.
[21] D. Zhou, W.B. Li, J. Guo, L.X. Pang, Z.M. Qi, T. Shao, H.D. Xie, Z.X. Yue, X. Yao, Structure, phase evolution, and microwave dielectric properties of $(Ag_{0.5}Bi_{0.5})(Mo_{0.5}W_{0.5})O_4$ ceramic with ultralow sintering temperature, Inorg. Chem. 53 (2014) 5712–5716.
[22] G.J. Redhammer, G. Roth, G. Amthauer, W. Lottermoser, On the crystal chemistry of olivine-type germanate compounds, $Ca_{1+x}M_{1-x}GeO_4$ (M^{2+} = Ca, Mg, Co, Mn), Acta Crystallogr. B 64 (2008) 261–271.
[23] A.J. Bosman, E.E. Havinga, Temperature dependence of dielectric constants of cubic ionic compounds, Phys. Rev. 129 (1963) 1593–1600.
[24] R.D. Shannon, Dielectric polarizabilities of ions in oxides and fluorides, J. Appl. Phys. 73 (1993) 348–366.
[25] S. George, P.S. Anjana, V.N. Deepu, P. Mohanan, M.T. Sebastian, Low-temperature sintering and microwave dielectric properties of Li_2MgSiO_4 Ceramics, J. Am. Ceram. Soc. 92 (2009) 11244–11249.
[26] H.W. Chen, H. Su, H.W. Zhang, T.C. Zhou, B.W. Zhang, J.F. Zhang, X.L. Tang, Low-temperature sintering and microwave dielectric properties of $(Zn_{1-x}Co_x)_2SiO_4$ ceramics, Ceram. Int. 40 (2014) 14655–14659.
[27] Y.C. Chen, Y.N. Wang, C.H. Hsu, Elucidating the dielectric properties of Mg_2SnO_4 ceramics at microwave frequency, J. Alloys. Compd. 509 (2011) 9650–9653.
[28] F. Shi, H. Dong, Correlation of crystal structure, dielectric properties and lattice vibration spectra of $(Ba_{1-x}Sr_x)(Zn_{1/3}Nb_{2/3})O_3$ solid solutions, Dalton Trans. 40 (2011) 6659–6667.
[29] D. Zhou, L.X. Pang, D.W. Wang, I.M. Reaney, $BiVO_4$ based high *k* microwave dielectric materials: a review, J. Mater. Chem. C 6 (2018) 9290–9313.
[30] H. Xiang, C. Li, Y. Tang, L. Fang, Two novel ultralow temperature firing microwave dielectric ceramics $LiMVO_6$ (M = Mo, W) and their chemical compatibility with metal electrodes, J. Eur. Ceram. Soc. 37 (2017) 3959–3963.
[31] J. Guo, D. Zhou, Y. Li, T. Shao, Z.M. Qi, B.B. Jin, H. Wang, Structure-property relationships of novel microwave dielectric ceramics with low sintering temperatures: $(Na_{0.5x}Bi_{0.5x}Ca_{1-x})MoO_4$, Dalton Trans. 43 (2014) 11888–11896.
[32] D.L. Rousseau, R.P. Bauman, S.P.S. Porto, Normal mode determination in crystals, J. Raman Spectrosc. 10 (1981) 253–290.
[33] I. Weber, U. Böttger, S.G. Pavlov, E.K. Jessberger, H.W. Hübers, Mineralogical and Raman spectroscopy studies of natural olivines exposed to different planetary environments, Planet. Space Sci. 104 (2014) 163–172.
[34] H.L. Zheng, Z.C. Zhang, J.G. Zhou, S.S. Yang, J. Zhao, Vibrational spectra of $CaGa_2O_4$, Ca_2GeO_4, $CaIn_2O_4$ and $CaSnO_3$ prepared by electrospinning, Appl. Phys. A-Mater. 108 (2012) 465–473.
[35] F. Shi, H. Dong, Vibrational modes and structural characteristics of $(Ba_{0.3}Sr_{0.7})[(Zn_xMg_{1-x})_{1/3}Nb_{2/3}]O_3$ solid solutions, Dalton Trans. 40 (2011) 11591–11598.
[36] C. Xing, J. Li, J. Wang, H. Chen, H. Qiao, X. Yin, Q. Wang, Z.M. Qi, F. Shi, Internal relations between crystal structures and intrinsic properties of nonstoichiometric $Ba_{1+x}MoO_4$ ceramics, Inorg. Chem. 57 (2018) 7121–7128.
[37] X.S. Lyu, L.X. Li, S. Zhang, H. Sun, B.W. Zhang, J.T. Li, M.K. Du, Crystal structure and microwave dielectric properties of novel (1-*x*)$ZnZrNb_2O_8$-*x*TiO_2 ceramics, Mater. Lett. 171 (2016) 129–132.
[38] J. Guo, D. Zhou, H. Wang, X. Yao, Microwave dielectric properties of (1-x)$ZnMoO_4$-xTiO_2 composite ceramics, J. Alloys Compd. 509 (2011) 5863–5865.
[39] C.L. Huang, C.L. Pan, S.J. Shium, Liquid phase sintering of $MgTiO_3$-$CaTiO_3$ microwave dielectric ceramics, Mater. Chem. Phys. 78 (2003) 111–115.